

This discussion paper is/has been under review for the journal *Climate of the Past* (CP). Please refer to the corresponding final paper in CP if available.

# Interhemispheric coupling and warm Antarctic interglacials

P. B. Holden<sup>1</sup>, N. R. Edwards<sup>1</sup>, E. W. Wolff<sup>2</sup>, N. J. Lang<sup>2</sup>, J. S. Singarayer<sup>3</sup>,  
P. J. Valdes<sup>3</sup>, and T. F. Stocker<sup>4</sup>

<sup>1</sup>Earth and Environmental Sciences, Open University, Milton Keynes, UK

<sup>2</sup>British Antarctic Survey, Cambridge, UK

<sup>3</sup>School of Geographical Sciences, University of Bristol, Bristol, UK

<sup>4</sup>Climate and Environmental Physics, University of Bern, Bern, Switzerland

Received: 27 November 2009 – Accepted: 4 December 2009 – Published: 17 December 2009

Correspondence to: P. B. Holden (p.b.holden@open.ac.uk)

Published by Copernicus Publications on behalf of the European Geosciences Union.

## Interhemispheric coupling and warm Antarctic interglacials

P. B. Holden et al.

Title Page

Abstract

Introduction

Conclusions

References

Tables

Figures

⏪

⏩

◀

▶

Back

Close

Full Screen / Esc

Printer-friendly Version

Interactive Discussion

## Abstract

Ice core evidence indicates that even though atmospheric CO<sub>2</sub> concentrations did not exceed ~300 ppm at any point during the last 800 000 years, East Antarctica was at least ~3–4 °C warmer than pre-industrial (CO<sub>2</sub> ~280 ppm) in each of the last four interglacials. During the previous three interglacials, this anomalous warming was short lived (~3 000 years) and apparently occurred before the completion of Northern Hemisphere deglaciation. Hereafter, we refer to these periods as “Warmer than Present Transients” (WPTs). We here present transient 800 kyr simulations using the intermediate complexity model GENIE-1 which suggest that WPTs could be explained as a consequence of the meltwater-forced slowdown of the Atlantic Meridional Overturning Circulation (AMOC) during glacial terminations. It is well known that a slowed AMOC would increase southern Sea Surface Temperature (SST) through the bipolar seesaw. Observational data supports this hypothesis, suggesting that the AMOC remained weak throughout the terminations preceding WPTs, strengthening rapidly at a time which coincides closely with peak Antarctic temperature. In order to investigate model and boundary condition uncertainty, we additionally present three ensembles of transient GENIE-1 simulations across Termination II (135 000 to 124 000 BP) and three snapshot HadCM3 simulations at 130 000 Before Present (BP). These simulations together reproduce both the timing and magnitude of WPTs, and point to the potential importance of an albedo feedback associated with West Antarctic Ice Sheet (WAIS) retreat.

## 1 Introduction

The AMOC transports a substantial amount of heat from South to North. If the AMOC is weakened through changes in surface buoyancy, Northern Atlantic cooling and Southern Atlantic warming is simulated in ocean models of various complexities (Stouffer et al., 2006). This effect, the bipolar seesaw, has been proposed (Stocker and Johnsen,

CPD

5, 2555–2575, 2009

## Interhemispheric coupling and warm Antarctic interglacials

P. B. Holden et al.

Title Page

Abstract

Introduction

Conclusions

References

Tables

Figures

⏪

⏩

◀

▶

Back

Close

Full Screen / Esc

Printer-friendly Version

Interactive Discussion

2003) to explain the interhemispheric teleconnection of abrupt millennial-scale shifts in glacial climate known as Dansgaard-Oeschger (DO) events (Dansgaard et al., 1993). We here propose that the bipolar seesaw may play a similarly important role in defining the characteristics of glacial terminations and the interglacials which follow them.

5 Antarctic temperature (Jouzel et al., 2007) and atmospheric methane (Loulergue et al., 2008) are illustrated in Fig. 1a. Numerous paleorecords (Carlson, 2008) reveal that the most recent termination (TI) exhibited rapid transitions in Northern Hemisphere climate, in approximate anti-phase with change in Antarctica (Blunier et al., 1998). Antarctica warmed slowly from  $\sim 18$  kyr BP to temperatures similar to pre-industrial at  
10  $\sim 12$  kyr BP, interrupted by the Antarctic Cold Reversal (ACR) at  $\sim 14$  kyr BP, a cooling event which has been interpreted as the southern analogue of the Bolling-Allerod Northern Hemisphere warming, both manifestations of a temporary resumption of Atlantic overturning (Blunier et al., 1998; Barker et al., 2009). Rapid increases in methane provide a proxy for rapid increases in Greenland temperature (Delmotte et al., 2004) and hence, according to this interpretation, for the resumption of overturning.  
15

In contrast, the three previous terminations (TII, TIII and TIV) exhibit a behaviour that is quite distinct from TI, although they display remarkable similarities to one another. In each case a transient spike in Antarctic temperature (WPT) of up to  $\sim 4^\circ\text{C}$  lasting  $\sim 3$  kyr is apparent at the start of the interglacial. Recent analysis (Sime et al.,  
20 2009) has revealed that the isotopic composition of East Antarctic ice is less sensitive to temperature change in a warm climate, consistent with even higher peak Antarctic temperatures during these interglacials (at least  $\sim 6^\circ\text{C}$  warmer than present day), though this work did not consider the warming mechanism of the bipolar seesaw that is addressed here. GCM simulations have thus far failed to produce a warmer Antarctica during the last interglacial (e.g. Montoya et al., 2000; Groll et al., 2005; Otto-Bliesner  
25 et al., 2006; Masson-Delmotte et al., 2009).

The second striking similarity between these earlier terminations is that the methane record does not exhibit the oscillatory behaviour that is apparent in TI, but rather displays a single rapid jump late in the termination (which we associate with a resumption

---

## Interhemispheric coupling and warm Antarctic interglacials

P. B. Holden et al.

---

[Title Page](#)[Abstract](#)[Introduction](#)[Conclusions](#)[References](#)[Tables](#)[Figures](#)[⏪](#)[⏩](#)[◀](#)[▶](#)[Back](#)[Close](#)[Full Screen / Esc](#)[Printer-friendly Version](#)[Interactive Discussion](#)

## Interhemispheric coupling and warm Antarctic interglacials

P. B. Holden et al.

of overturning). In each case this methane jump coincides closely with the peak in Antarctic temperature. Furthermore, each methane jump corresponds to an abrupt shift in Chinese speleothem  $\delta^{18}\text{O}$  (Wang et al., 2001; Cheng et al., 2006, 2009), a proxy for Asian Monsoon precipitation, further suggesting a role for the bipolar seesaw during terminations (Kelly et al., 2006). A recent climate model simulation which included a parameterisation of Greenland melt at 126 kyr BP predicted year-round warming of  $0.5^\circ\text{C}$  in Antarctica, implicating the bipolar seesaw as a possible driver of transient warmth in MIS 5.5 (Masson-Delmotte et al., 2009). It has recently been suggested that the suppression of DO events (which would cool Antarctica) enables terminations to progress unchecked (Wolff et al., 2009). Here we propose that if overturning remains weakened throughout the termination, the system will progress to a WPT state. Although global radiative forcing is similar to modern in the early interglacial, weakened overturning leads to conditions in Antarctica which are significantly warmer than modern. The resumption of overturning, associated with the cessation of deglaciation meltwater, subsequently cools Antarctica to conditions that are comparable to present day.

In order to examine the temporal history of Northern Hemisphere meltwater feedbacks on Antarctic climate, and evaluate the modelling and boundary condition uncertainty, we have performed three sets of simulations:

- (i) Two transient 800 kyr simulations with GENIE-1, one which includes the effects of glacial meltwater on ocean circulation and one which neglects this feedback. These simulations provide a long time-series comparison between observations and modelling and an assessment of the role of meltwater in determining transient Northern Atlantic and Antarctic temperatures.
- (ii) Three ensembles of GENIE-1 transient simulations over glacial termination TII. These ensembles enable quantification of both modelling and boundary condition uncertainties, including an evaluation of potential WAIS retreat feedbacks.

[Title Page](#)[Abstract](#)[Introduction](#)[Conclusions](#)[References](#)[Tables](#)[Figures](#)[Back](#)[Close](#)[Full Screen / Esc](#)[Printer-friendly Version](#)[Interactive Discussion](#)

- (iii) Three equilibrium simulations with HadCM3 at 130 000 BP, performed to investigate the robustness of the conclusions derived from GENIE-1, in particular with respect to its simplified atmosphere and snow models.

## 2 Methods

### 2.1 GENIE-1

The intermediate complexity model GENIE-1 has been extensively applied to investigations of the thermohaline circulation (Marsh et al., 2004) and provides the computational efficiency required to perform large ensembles and quantify model uncertainty. The physical model comprises a 3-D frictional geostrophic ocean with eddy-induced and isopycnal mixing coupled to a 2-D fixed wind-field energy-moisture balance atmosphere and a dynamic and thermodynamic sea-ice component (Edwards and Marsh, 2005). These are coupled to a minimum spatial model of vegetation carbon, soil carbon and soil water storage (Williamson et al., 2006). The model configuration is as described in Lenton et al. (2006), with adjustments to the parameterisation of Outgoing Longwave Radiation (OLR) and the inclusion of orography feedbacks for surface processes as described in Holden et al. (2009).

Changing atmospheric CO<sub>2</sub> is prescribed from ice core records (Luethi et al., 2008). We apply the orbital forcing of Berger (1978). Transient Laurentide and Eurasian Ice Sheets are represented by interpolating the spatial distribution of Ice-4G (Peltier, 1994) onto the benthic  $\delta^{18}\text{O}$  record (Lisiecki and Raymo, 2005). We derive three variables for each grid cell representing (a) the threshold value  $\delta^{18}\text{O}_{\text{th}}$  at which the grid cell becomes ice covered, (b) the present-day orography  $h_0$  and (c) the incremental orography  $h_1$  at maximum attainable ice thickness. When  $\delta^{18}\text{O} > \delta^{18}\text{O}_{\text{th}}$ , the height of the ice surface  $h$

## Interhemispheric coupling and warm Antarctic interglacials

P. B. Holden et al.

Title Page

Abstract

Introduction

Conclusions

References

Tables

Figures

⏪

⏩

◀

▶

Back

Close

Full Screen / Esc

Printer-friendly Version

Interactive Discussion

at each cell is given by the saturating relationship

$$h = h_0 + h_1 \frac{(\delta^{18}\text{O} - \delta^{18}\text{O}_{\text{th}})}{(\delta^{18}\text{O} - \delta^{18}\text{O}_{\text{th}} + k)} \quad (1)$$

where  $h_1$  is defined to give the 4G ice sheet height  $h_{\text{LGM}}$  at  $\delta^{18}\text{O}_{\text{LGM}}$ . The threshold for ice cover  $\delta^{18}\text{O}_{\text{th}}$  is derived from Ice-4G reconstructions at 1 kyr intervals from 21 kyr BP to present. The constant  $k$  is fitted to approximate a linear relationship between global ice volume and  $\delta^{18}\text{O}$ . The relationship in Eq. (1) is assumed to hold throughout the 800 kyr record so that the value of  $\delta^{18}\text{O}$  at any point in time defines the spatial distribution and orography of the ice sheets globally.

Changing ice volume is translated into meltwater fluxes at each grid cell, routed to the ocean assuming modern topography, with accumulating ice represented by reduced run-off. This ensures that freshwater fluxes are spatially and temporally consistent with the representation of the ice sheets, and avoids the problems associated with an unrealistic treatment of salt compensation which is responsible for much of the uncertainty in the far-field response to freshwater forcing (Stocker et al., 2007). Only the Laurentide and Eurasian Ice Sheets, which account for  $\sim 80\%$  of global ice-sheet change (Peltier, 2004), are allowed to change. This eliminates the potentially confounding effects of assuming synchronous Antarctic meltwater on ocean circulation (but neglects possible WAIS meltwater feedbacks); it is well known that millennial-scale Southern and Northern Hemisphere changes are likely to be out of phase (Blunier et al., 1998). A multiple (FFX) is applied to the freshwater forcing to correct for isostatic depression at the ice-bedrock interface (which we do not model) and for the assumption of a fixed land-sea mask; each of these simplifications would otherwise produce a  $\sim 20\%$  underestimation of ice-sheet volume.

### 2.1.1 Transient GENIE-1 800 kyr simulations

The 800 kyr simulations apply the “traceable” GENIE-1 parameterisation, the climatology of which is discussed in detail elsewhere (Lenton et al., 2006). The equilibrium

## Interhemispheric coupling and warm Antarctic interglacials

P. B. Holden et al.

Title Page

Abstract

Introduction

Conclusions

References

Tables

Figures

⏪

⏩

◀

▶

Back

Close

Full Screen / Esc

Printer-friendly Version

Interactive Discussion



## Interhemispheric coupling and warm Antarctic interglacials

P. B. Holden et al.

Title Page

Abstract

Introduction

Conclusions

References

Tables

Figures

⏪

⏩

◀

▶

Back

Close

Full Screen / Esc

Printer-friendly Version

Interactive Discussion



climate sensitivity of this parameterisation to a doubling of  $\text{CO}_2$  is  $3.4^\circ\text{C}$ . Although the default OLR parameterisation is applied ( $K_{\text{LW}0}=0\text{Wm}^{-2}$ ,  $K_{\text{LW}1}=0\text{Wm}^{-2}\text{K}^{-1}$ , Holden et al., 2009), our climate sensitivity is slightly higher than the value of  $3.2^\circ\text{C}$  in the configuration of Lenton et al. (2006) due to the increased snow albedo feedback that arises from the inclusion of a lapse rate for surface processes. Two simulations are performed:  $G_{\text{FW}}$ , which includes the effects of glacial meltwater on ocean circulation (FFX=1.5), and  $G_{\text{NFW}}$  which neglects this feedback (FFX=0).

### 2.1.2 Transient GENIE-1 Termination II ensembles

Three ensembles of transient simulations over TII (providing approximate analogues for TIII and TIV) are performed, differing in the boundary conditions applied in order to investigate uncertainties in forcing. The ensembles each vary 26 parameters over wide ranges. Ensemble members are weakly constrained to produce plausible modern and LGM climate states by applying the 480 member LPC parameter set (Holden et al., 2009). The LPC parameters produce modern-plausible global average Surface Air Temperature (SAT, expressed as sea-level equivalent throughout), Atlantic overturning strength, Antarctic sea-ice coverage and land carbon storage, with distributions that are approximately centred on observations, and are additionally constrained to simulate plausible LGM Antarctic cooling (of  $6\text{--}12^\circ\text{C}$ ). The approach is designed to quantify model error by allowing parametric uncertainty to dominate over structural error. The ensemble members exhibit a wide range of feedback strengths which generally encompass the range of large-scale GCM responses to  $2\times\text{CO}_2$  and LGM forcing, with a distribution for climate sensitivity of  $3.8\pm 0.6^\circ\text{C}$  and for LGM globally averaged cooling of  $5.9\pm 1.2^\circ\text{C}$ .

The three ensembles are:  $E_{\text{FW}}$  which includes the impact of meltwater on ocean circulation and allows for uncertainty in the strength of this feedback by varying (in addition to 25 other parameters) FFX in the range 1 to 2,  $E_{\text{NFW}}$  which neglects the role of meltwater (FFX=0 in all ensemble members) and  $E_{\text{WAIS}}$  which is identical to  $E_{\text{FW}}$  except that the WAIS is replaced with land at sea-level. Ice-sheet models (Pollard and

---

## Interhemispheric coupling and warm Antarctic interglacials

P. B. Holden et al.

---

Title Page

Abstract

Introduction

Conclusions

References

Tables

Figures

⏪

⏩

◀

▶

Back

Close

Full Screen / Esc

Printer-friendly Version

Interactive Discussion

DeConto, 2009) have simulated substantial WAIS retreat driven by sea-level rise at terminations (neglecting the additional bipolar forcing addressed here). Although there is no direct evidence for WAIS retreat during the last interglacial, borehole constrained dynamical modelling of the Greenland Ice Sheet indicated that MIS 5 sea-level rise can only be explained with a contribution from WAIS retreat (Tarasov and Peltier, 2003). We capture the uncertainty associated with the degree and timing of potential WAIS retreat through the two extreme boundary conditions of  $E_{FW}$  and  $E_{WAIS}$ .

Transient  $CO_2$ , orbit and ice sheets are applied as for the long simulations, except that the benthic  $\delta^{18}O$  record is linearised across the termination to produce an approximately constant ( $\pm 20\%$ ) meltwater pulse, eliminating the oscillatory behaviour simulated during TII in the 800 kyr simulation (see Fig. 1c). This oscillatory behaviour is not apparent in observations and is largely a consequence of translating the temporal signal in the gradient of benthic  $\delta^{18}O$  into global ice-sheet change. The meltwater pulse commences at 135 000 BP and lasts for  $\sim 7600$  years with an average of  $\sim 0.14$  Sv, equivalent to 91 m sea level, but varying between ensemble members ( $\sim 0.09$  to 0.18 Sv) through the freshwater scaling parameter FFX. Simulations are spun-up to equilibrium at 135 000 BP and run for 11 000 years.

## 2.2 HadCM3 snapshot simulations

The snapshot simulations are performed using the Hadley Centre coupled model HadCM3 (Gordon et al., 2000), a coupled atmosphere ( $2.5^\circ \times 3.75^\circ \times 19$  vertical levels) / ocean ( $1.25^\circ \times 1.25^\circ \times 20$  vertical levels) model which does not require flux adjustments. Boundary conditions are ( $H_M$ ) pre-industrial, ( $H_{NFW}$ ) 130 000 BP orbit and greenhouse gases ( $CO_2$  256 ppm,  $CH_4$  506 ppb,  $N_2O$  239 ppb) with modern ice sheets and no meltwater flux, ( $H_{FW}$ ) as  $H_{NFW}$  with 1 Sv North Atlantic hosing (large enough to ensure collapse on timescales which can be practically simulated) and ( $H_{WAIS}$ ) as  $H_{FW}$  with WAIS replaced by land at 200 m. Simulations are run for 200 years and averaged over the last 30 years.

### 3 Results

#### 3.1 800kyr GENIE-1 Transient Simulations

Figure 1b compares 800 kyr records of i) modelled Antarctic Surface Air Temperature (SAT) anomaly with DOME C (Jouzel et al., 2007) and ii) modelled SST anomaly with a North Atlantic planktonic  $\delta^{18}\text{O}$  record (Venz et al., 1999) which we have mapped onto the LR04 timescale (Lisiecki and Raymo, 2005). Model data are from the simulation  $G_{\text{FW}}$  (which includes meltwater forcing). We note the generally good agreement with both sets of observational data, with the exception of the marked failure to predict the existence of Antarctic WPTs. A similar discrepancy is not apparent in the North Atlantic record and we infer that WPTs are likely driven by an absent Southern Hemisphere forcing. MIS 7 is particularly interesting in this regard as the  $\delta^{18}\text{O}$  record suggest that substantial Northern Hemisphere ice sheets remained in place during this interglacial, so that temperatures  $\sim 2^\circ\text{C}$  higher than pre-industrial again suggest the WPT warming was localised to the Southern Hemisphere. For completeness we note that orbitally-forced summer warming is simulated at high northern latitudes during the Eemian, with maximum summer warming (averaged over all grid points north of  $62^\circ\text{N}$ ) peaking at  $3.5^\circ\text{C}$  in 126 000 BP.

The first plot in Fig. 1c is the 350 kyr DOME F temperature record (Kawamura et al., 2007), chosen as it lies south of the Atlantic ( $77^\circ\text{S}$ ,  $39^\circ\text{E}$ ) and may be expected to be more strongly influenced by AMOC changes than DOME C ( $75^\circ\text{S}$ ,  $123^\circ\text{E}$ ). In addition to the WPTs, and the warm spike in the early Holocene, three interstadials at DOME F are warmer than modern at 317, 218 and 200 kyr BP. We note that these apparent temperature differences between DOME C and DOME F may alternatively reflect spatial variations in the seasonality of precipitation in a warm Antarctica (Sime et al., 2009).

Antarctic SAT and SST meltwater anomalies ( $G_{\text{FW}} - G_{\text{NFW}}$ , i.e. the differences in temperature when meltwater is imposed) are plotted in Fig. 1c and reflect the impact of meltwater on ocean circulation and heat transport. The SAT meltwater anomaly

## Interhemispheric coupling and warm Antarctic interglacials

P. B. Holden et al.

Title Page

Abstract

Introduction

Conclusions

References

Tables

Figures



Back

Close

Full Screen / Esc

Printer-friendly Version

Interactive Discussion



displays the millennial variability apparent in observations; the SST meltwater anomaly exhibits a similar temporal behaviour, though variability is suppressed by high-latitude sea ice during glacial periods. The SST meltwater spikes coincide very closely with spikes in DOME F temperature. Late Pleistocene LR04 age-model uncertainty (the age model which defines the meltwater timing through the gradient of the benthic  $\delta^{18}\text{O}$ ) is estimated at 4 kyr (Lisiecki and Raymo, 2005).

### 3.2 GENIE-1 ensembles of transient simulations over Termination II

Although there is strong chronological similarity between observed and simulated warming, the magnitude of Antarctic SAT spikes in the single 800 kyr simulation  $G_{\text{FW}}$  ( $\sim 1.5^\circ\text{C}$ , Fig. 1c) is insufficient to explain the observed warmings of  $\sim 4^\circ\text{C}$  above present (Fig. 1b). Quantification of the discrepancy requires an assessment of modelling errors; we apply an ensemble methodology to ascertain the most probable model response and quantify uncertainty.

The 480 meltwater-forced ensemble members  $E_{\text{FW}}$  universally exhibited weakened overturning during the termination (average weakening at 128 000 BP of  $9\pm 5\text{ Sv}$  with respect to modern). Antarctic SAT at 128 000 BP is  $>0.5^\circ\text{C}$  warmer than pre-industrial in 110 of these simulations, all of which exhibited a collapse of overturning (peak overturning  $<6\text{ Sv}$  north of  $44^\circ\text{N}$ ), demonstrating that AMOC collapse is required for significant Antarctic warming in GENIE-1. We confine analysis to the 174 parameter sets with maximum overturning  $<6\text{ Sv}$  to quantify the range of response.

Figure 2a illustrates the meltwater-forced SST anomaly at 128 500 BP ( $E_{\text{FW}} - E_{\text{NFW}}$ , i.e. the ensemble-averaged change in SST when meltwater is imposed) and displays the characteristic behaviour of the bipolar seesaw, although certain atmospheric feedbacks, such as the southward shift of the ITCZ, cannot be captured by the fixed-wind field EMBM. South of  $62^\circ\text{S}$ , ensemble-averaged SST warming of  $0.4\pm 0.3^\circ\text{C}$  is simulated (uncertainties are expressed as  $1\sigma$  ensemble standard deviations throughout). Modern observations indicate that basal melt rates at the WAIS grounding line increase by  $\sim 1\text{ m yr}^{-1}$  for a  $0.1^\circ\text{C}$  increase in SST (Rignot and Jacobs, 2002), suggesting that

## Interhemispheric coupling and warm Antarctic interglacials

P. B. Holden et al.

Title Page

Abstract

Introduction

Conclusions

References

Tables

Figures

⏪

⏩

◀

▶

Back

Close

Full Screen / Esc

Printer-friendly Version

Interactive Discussion



---

**Interhemispheric  
coupling and warm  
Antarctic  
interglacials**P. B. Holden et al.

---

the simulated warming may be significant for WAIS instability – ice-sheet modelling has indicated that a  $10 \text{ m yr}^{-1}$  increase in Antarctic basal melt rates leads to sea level rise of  $\sim 25 \text{ cm}$  per century (Huybrechts and de Wolde, 1999). The ensemble design allows a wide range of sea-ice responses, with annual average Antarctic sea ice extent increasing by 9–15 million  $\text{km}^2$  under LGM forcing and decreasing by 5–9 million  $\text{km}^2$  under  $2\times\text{CO}_2$  forcing (Holden et al., 2009). Meltwater-forced reduction in Antarctic sea-ice area at 128 500 BP is  $2.7\pm 1.6$  million  $\text{km}^2$ . The simulated retreat of Antarctic sea ice is consistent with the southerly shift of productivity inferred from barium rain rates during MIS5.5 which can only be explained by a reduction in Antarctic sea ice (Nuernberg et al., 1997). The ensemble member with the largest meltwater-induced loss of Antarctic sea ice (7.9 million  $\text{km}^2$ ) is associated with an Antarctic SAT  $2.6^\circ\text{C}$  warmer than modern. Thus the possibility that WPTs could be explained without a substantial WAIS retreat feedback appears unlikely but cannot be ruled out.

Figure 2b–d illustrates ensemble-averaged SAT anomalies at 128 500 BP with respect to an equilibrium ensemble  $E_M$  forced with pre-industrial boundary conditions. In the absence of meltwater forcing (Fig. 2b), SAT is cooler than modern (despite slightly higher atmospheric  $\text{CO}_2$  concentrations of  $\sim 285 \text{ ppm}$ ), reflecting cooling due to the inferred remnant of the Laurentide ice sheet at this time. Meltwater forcing (Fig. 2c) increases Antarctic SAT by  $1.6\pm 1.0^\circ\text{C}$  (to  $0.5\pm 1.0^\circ\text{C}$  warmer than modern). These simulations suggest the possibility of a bipolar-induced spatial temperature profile across East Antarctica, peaking in the vicinity of DOME F, qualitatively consistent with the observed temperature difference between DOME F and DOME C during the three warm DOME F interstadials. The removal of WAIS (Fig. 2d) introduces further Antarctic warming of  $2.3\pm 1.2^\circ\text{C}$  (to  $2.8\pm 1.7^\circ\text{C}$  warmer than modern) arising from widespread loss of West Antarctic summer snow cover and reduced albedo.

Figure 2e summarises the temporal development of ensemble-averaged Antarctic SAT under the three forcing scenarios. We do not regard WAIS retreat early in the termination as realistic; in the absence of a dynamic ice-sheet model we have simply assumed WAIS is absent throughout the  $E_{\text{WAIS}}$  run, so the temporal behaviour

[Title Page](#)[Abstract](#)[Introduction](#)[Conclusions](#)[References](#)[Tables](#)[Figures](#)[⏪](#)[⏩](#)[◀](#)[▶](#)[Back](#)[Close](#)[Full Screen / Esc](#)[Printer-friendly Version](#)[Interactive Discussion](#)

## Interhemispheric coupling and warm Antarctic interglacials

P. B. Holden et al.

Title Page

Abstract

Introduction

Conclusions

References

Tables

Figures

⏪

⏩

◀

▶

Back

Close

Full Screen / Esc

Printer-friendly Version

Interactive Discussion

would more reasonably be described by a transition from the  $E_{FW}$  ensemble towards the  $E_{WAIS}$  ensemble (reconciling the rate of warming with observations). Maximum overturning is also illustrated. In contrast to paleoclimatic evidence suggesting that glacial (LGM) overturning was weaker than today (MacManus et al., 2004), GENIE-1 ensemble-averaged overturning is stronger in the glacial state. However, this change is of unclear sign, with 63 of the 174 simulations displaying a weakened overturning at 135 000 BP (ensemble average  $0.9 \pm 2.6$  Sv relative to modern). The resumption of overturning is  $\sim 1$  500 years later than the methane jump (Fig. 1a), possibly attributable to differences in the relationship between  $\delta^{18}O$  and ice sheets at TII (we apply the relationship derived from TI data), although the delayed resumption is consistent with coral reef evidence (Thomas et al., 2009) which indicates that sea-level rise during TII occurred earlier than suggested by the orbitally-tuned benthic  $\delta^{18}O$  stack (Lisiecki and Raymo 2005) used to derive meltwater forcing.

The  $E_{NFW}$  ensemble distribution of SAT (Fig. 2f) illustrates that no point in our parameter space is capable of reconciling GENIE-1 with observations in the absence of substantial AMOC weakening (though we note that  $\sim 10\%$  of the simulations exhibit AMOC collapse in the absence of meltwater forcing). However, the two extreme boundary conditions represented by the distributions of  $E_{FW}$  and  $E_{WAIS}$  encompass the observational estimate of  $\sim 4^\circ C$  warming. Although we do not rule out the possibility that the bipolar seesaw could reconcile the discrepancy without a substantial WAIS feedback, we note that the observed Antarctic warming of  $\sim 2^\circ C$  which persists after the resumption of overturning can only be reconciled in the GENIE-1 ensembles with the assumption of some WAIS retreat (or alternatively with an overturning that remains weakened throughout the interglacial - the AMOC does not recover from its collapsed state in 19 of the 174 simulations).

### 3.3 HadCM3 Eemian simulations

In order to investigate the robustness of the GENIE-1 ensembles, in particular with regard to the simplified atmosphere and snow models, we performed four equilibrium

HadCM3 simulations. Hosing induces AMOC collapse and results in statistically significant warming of  $\sim 0.2\text{--}0.5^\circ\text{C}$  in summer (DJF) SST in the Weddell and Ross Seas (Fig. 3a), accompanied by a reduction in Antarctic summer sea-ice extent and depth. A multi-model hosing ensemble (0.1 Sv, modern boundary conditions), performed to investigate inter-model uncertainty in response to hosing, also simulated warming in the Weddell Sea, apparently a consequence of enhanced deep convection and reduced sea ice (Stouffer et al., 2006).

In the absence of meltwater and ice-sheet forcing (Fig. 3b) HadCM3 fails to predict significant Antarctic SAT warming (though orbitally forced summer warming of  $3.0^\circ\text{C}$  is simulated in Greenland). With freshwater hosing (Fig. 3c), precipitation-weighted SAT increases by  $2.2^\circ\text{C}$  at DOME F and  $1.4^\circ\text{C}$  at DOME C, supporting GENIE-1 (annual-average Antarctic warming of  $1.6\pm 1.0^\circ\text{C}$ ). The removal of WAIS (Fig. 3d) increases the precipitation-weighted SAT anomaly to  $4.9^\circ\text{C}$  at DOME F and to  $5.0^\circ\text{C}$  at DOME C, arising from increased summer precipitation together with warming which is greatest in summer when widespread West Antarctic snow melt is simulated. The  $H_{\text{FW}}$  and  $H_{\text{WAIS}}$  simulations encompass observed WPT warming. As the GENIE-1 ensemble parameterisations were designed to provide an unbiased estimate of the uncertainty associated with large-scale processes,  $E_{\text{FW}}$  and  $E_{\text{WAIS}}$  Antarctic SAT variability of  $\pm 1.0^\circ\text{C}$  and  $\pm 1.7^\circ\text{C}$  provide indicative lower-bound measures of the parametric uncertainty in these single HadCM3 simulations.

## 4 Summary and conclusions

In summary we have demonstrated that both the chronology and magnitude of modelled Antarctic temperature over the last three glacial cycles can be reconciled with observations through the introduction of meltwater forcing during terminations, likely amplified by an albedo feedback resulting from WAIS retreat. We do not conclude that complete WAIS retreat is necessary to explain the discrepancy, but apply the extreme boundary conditions of modern and absent WAIS to span the possible range

## Interhemispheric coupling and warm Antarctic interglacials

P. B. Holden et al.

Title Page

Abstract

Introduction

Conclusions

References

Tables

Figures

⏪

⏩

◀

▶

Back

Close

Full Screen / Esc

Printer-friendly Version

Interactive Discussion

of response. We are not aware of other potential feedbacks that might explain  $\sim 4^{\circ}\text{C}$  warming across East Antarctica.

Several other points in the DOME F record are suggestive of a meltwater-forced bipolar signal, in particular the three anomalously warm interstadials which were apparently cooler at DOME C. During the previous three terminations, the bipolar seesaw would have warmed Antarctica throughout the deglaciation, with WAIS retreat occurring at some point, presumably late in the termination as interglacial conditions were approached. In contrast, the resumption of overturning during the Bolling-Allerod/ACR cooled Antarctica towards the end of T1, potentially preventing further southern warming though stabilisation of the WAIS.

## References

- Barker, S., Diz, P., Vautravers, M. J., Pike, J., Knorr, G., Hall, I. R., and Broecker, W. S.: Interhemispheric Atlantic seesaw response during the last deglaciation, *Nature*, 457, 1097–1103, 2009.
- Berger, A.: Long term variations of caloric insolation resulting from the Earth's orbital elements, *Quaternary Res.*, 9, 139–167, 1978.
- Blunier, T., Chappellaz, J., Schwander, J., Dällenbach, A., Stauffer, B., Stocker, T. F., Raynaud, D., Jouzel, J., Clausen, H. B., Hammer, C. U., and Johnsen, S. J.: Asynchrony of Antarctic and Greenland climate change during the last glacial period, *Nature*, 394, 739–743, 1998.
- Carlson, A. E.: Why there was not a Younger Dryas-like event during the Penultimate Deglaciation, *Quaternary Sci. Rev.*, 27, 882–887, 2008.
- Cheng, H., Edwards, R. L., Wang, Y., Kong, X., Ming, Y., Kelly, M. J., Wang, X., Gallup, C. D., and Liu, W.: A penultimate glacial monsoon record from Hulu Cave and two-phase glacial terminations, *Geology*, 34, 217–220, 2006.
- Cheng, H., Edwards, R. L., Broecker, W. S., Denton, G. H., Kong, X., Wang, Y., Zhang, R., and Wang, X.: Ice age terminations, *Science*, 326, 248–251, 2009.

## Interhemispheric coupling and warm Antarctic interglacials

P. B. Holden et al.

Title Page

Abstract

Introduction

Conclusions

References

Tables

Figures

◀

▶

◀

▶

Back

Close

Full Screen / Esc

Printer-friendly Version

Interactive Discussion

---

**Interhemispheric  
coupling and warm  
Antarctic  
interglacials**P. B. Holden et al.

---

- Dansgaard, W., Johnsen, S. J., Clausen, H. B., Dahl-Jensen, D., Gundestrup, N. S., Hammer, C. U., Hvidberg, C. S., Steffensen, J. P., Svelnbjörnsdottir, A. E., Jouzel, J., and Bond, G.: Evidence for general instability of past climate from a 250-kyr ice-core record, *Nature*, 364, 218–220, 1993.
- 5 Delmotte, M., Chappellaz, J., Brook, E., Yiou, P., Barnola, J. M., Goujon, C., Raynaud, D., and Lipenkov, V. I.: Atmospheric methane during the last four glacial-interglacial cycles: rapid changes and their link with Antarctic temperature, *J. Geophys. Res.*, 109, D12104, doi:10.1029/2003JD004417, 2004.
- Edwards, N. R. and Marsh, R.: Uncertainties due to transport-parameter sensitivity in an efficient 3-D ocean-climate model, *Clim. Dynam.*, 24, 415–433, 2005.
- 10 Gordon, C., Cooper, C., Senior, C. A., Banks, H., Gregory, J. M., Johns, T. C., Mitchell, J. F. B., and Wood, R. A.: The simulation of SST, sea ice extents and ocean heat transports in a version of the Hadley Centre coupled model without flux adjustments, *Clim. Dynam.*, 16, 147–168, 2000.
- 15 Groll, N., Widmann, M., Jones, J. M., Kaspar F., and Lorenz, S. J.: Simulated relationships between regional temperatures and large-scale circulation: 125 kyr BP (Eemian) and the preindustrial period, *J. Climate*, 18, 4032–4045, 2005.
- Holden, P. B., Edwards, N. R., Oliver, K. I. C., Lenton, T. M., and Wilkinson, R. D.: A probabilistic calibration of climate sensitivity and terrestrial carbon change in GENIE-1, *Clim. Dynam.*, <http://www.springerlink.com/content/x112908857p234h5/>, doi:10.1007/s00382-009-0630-8, 2009.
- 20 Huybrechts, P. and de Wolde, J.: The dynamic response of the Greenland and Antarctic ice sheets to multiple-century climate warming, *J. Climate*, 8, 2169–2188, 1999.
- Jouzel, J., Masson-Delmotte, V., Cattani, O., Dreyfus, G., Falourd, S., Hoffman, G., Minster, B., Nouet, J., Barnola, J. M., Chappellaz, J., Fischer, H., Gallet, J. G., Johnsen, S., Leuenberger, M., Loulergue, L., Luethi, D., Oerter, H., Parrenin, F., Raisbeck, G., Raynaud, D., Schilt, A., Schwander, J., Selmo, E., Souchez, R., Spahni, R., Stauffer, B., Steffensen, J.P., Stenni, B., Stocker, T. F., Tison, J. L., Werner, M., and Wolff, E. W.: Orbital and Millennial Antarctic climate variability over the past 800,000 years, *Science*, 317, 793–796, 2007.
- 25 Kawamura, K., Parrenin, F., Lisiecki, L., Uemura, R., Vimeux, F., Severinghaus, J. P., Hutterli, M. A., Nakazawa, T., Aoki, S., Jouzel, J., Raymo, M., Matsumoto, K., Nakata, H., Motoyama, H., Fujita, S., Goto-Azuma, K., Fujii, Y., and Watanabe, O.: Northern Hemisphere forcing of climatic cycles in Antarctica over the past 360,000 years, *Nature*, 448, 912–916, 2007.
- 30

[Title Page](#)[Abstract](#)[Introduction](#)[Conclusions](#)[References](#)[Tables](#)[Figures](#)[⏪](#)[⏩](#)[◀](#)[▶](#)[Back](#)[Close](#)[Full Screen / Esc](#)[Printer-friendly Version](#)[Interactive Discussion](#)

**Interhemispheric  
coupling and warm  
Antarctic  
interglacials**

P. B. Holden et al.

Title Page

Abstract

Introduction

Conclusions

References

Tables

Figures

◀

▶

◀

▶

Back

Close

Full Screen / Esc

Printer-friendly Version

Interactive Discussion



- Kelly, M. J., Edawrds, R. L., Cheng, H., Yuan, D., Cai, Y., Zhang, M., Lin, Y., and An, Z.: High resolution characterisation of the Asian Monsoon between 146,000 and 99,000 years B.P. from Donge Cave, China and global correlation of events surrounding Termination II, *Palaeogeogr. Palaeoclimatol.*, 236, 20–38, 2006.
- 5 Lenton, T. M., Williamson, M. S., Edwards, N. R., Marsh, R., Price, A. R., Ridgwell, A. J., Shepherd, J. G., Cox, S. J., and The GENIE team: Millennial timescale carbon cycle and climate change in an efficient Earth system model, *Clim. Dynam.*, 26, 687–711, 2006.
- Lisiecki, L. E. and Raymo, M. E.: A Pliocene-Pleistocene stack of 57 globally distributed benthic  $\delta^{18}\text{O}$  records, *Paleoceanography*, 20, PA1003, doi:10.1029/2004PA001071, 2005.
- 10 Loulergue, L., Schilt, A., Spahni, R., Masson-Delmotte, V., Blunier, T., Lemieux, B., Barnola, J.-M., Raynaud, D., Stocker, T. F., and Chappellaz, J. M.: Orbital and millennial scale features of atmospheric  $\text{CH}_4$  over the last 800,000 years, *Nature*, 453, 383–386, 2008.
- Luethi, D., Le Floch, M., Bereiter, B., Blunier, T., Barnola, J.-M., Siegenthaler, U., Raynaud, D., Jouzel, J., Fischer, H., Kawamura, K., and Stocker, T. F.: High-resolution carbon dioxide concentration record 650,000–800,000 years before present, *Nature*, 453, 379–382, 2008.
- 15 Marsh, R., Yool, A., Lenton, T. M., Gulamali, M. Y., Edwards, N. R., Shepherd, J. G., Krznaric, M., Newhouse, S., and Cox, S. J.: Bistability of the thermohaline circulation identified through comprehensive 2-parameter sweeps of an efficient climate model, *Clim. Dynam.*, 23, 761–777, 2004.
- 20 Masson-Delmotte, V., Stenni, B., Pol, K., Braconnot, P., Cattani, O., Falourd, S., Kageyama, M., Jouzel, J., Landais, A., Minster, B., Barnola, J. M., Chappellaz, J., Krinner, G., Johnsen, S., Röthlisberger, R., Hansen, J., Mikolajewicz, U., and Otto-Bliesener, B.: EPICA Dome C record of glacial and interglacial intensities, *Quat. Sci. Rev.*, <http://dx.doi.org/10.1016/j.quascirev.2009.09.030>, doi:10.1016/j.quascirev.2009.09.030, 2009.
- 25 McManus, J. F., Francois, R., Gherardi, J.-M., Keigwin, L. D., and Brown-Leger, S.: Collapse and rapid resumption of Atlantic meridional circulation linked to deglacial climate changes, *Nature*, 428, 834–837, 2004.
- Montoya, M., von Storch, H., and Crowley, T. J.: Climate simulation for 125 kyr BP with a coupled ocean-atmosphere general circulation model, *J. Clim.*, 13, 1057–1072, 2000.
- 30 Nuernberg, C. C., Bohrmann, G., and Schlueter, M.: Barium accumulation in the Atlantic sector of the Southern Ocean: results from 190,000 year records, *Paleoceanography*, 12, 594–603, 1997.

---

**Interhemispheric  
coupling and warm  
Antarctic  
interglacials**P. B. Holden et al.

---

- Otto-Bliesner, B. L., Marshall, S. J., Overpeck, J. T., Miller, G. H., Hu, A., and CAPE Last Interglacial Project Members: Simulating Arctic climate warmth and icefield retreat in the last interglaciation, *Science*, 311, 1751–1753, 2006.
- Peltier, W. R.: Ice age paleotopography, *Science*, 265, 195–201, 1994.
- 5 Peltier, W. R.: Global glacial isostasy and the surface of the ice-age earth: the ICE-5G (VM2) model and GRACE, *Annu. Rev. Earth Pl. Sc.*, 32, 111–149, 2004.
- Pollard, D. and DeConto, R. M.: Obliquity-paced Pliocene West Antarctic ice sheet oscillations, *Nature*, 457, 329–333, 2009.
- Rignot, E. and Jacobs S. S.: Rapid bottom melting widespread near Antarctic ice sheet ground-  
10 ing lines, *Science*, 296, 2020–2023, 2002.
- Sime, L. C., Wolff, E. W., Oliver, K. I. C., and Tindall, J. C.: Evidence for warmer interglacials in East Antarctic ice cores, *Nature*, 462, 342–345, 2009.
- Stocker, T. F. and Johnsen, S. F.: A minimum thermodynamic model for the bipolar seesaw, *Paleoceanography*, 18, 1087, doi:10.1029/2003PA000920, 2003.
- 15 Stocker, T. F., Timmermann, A., Renold, M., and Timm, O.: Effects of salt compensation on the climate model response in simulations of large changes of the Atlantic Meridional Overturning Circulation, *J. Clim.*, 20, 5912–5928, 2007.
- Stouffer, R. J., Yin, J., Gregory, J. M., Dixon, K. W., Spelman, M. J., Hurlin, W., Weaver, A. J., Eby, M., Flato, G. M., Hasumi, H., Hu, A., Jungclaus, J. H., Kamenkovich, I. V., Levermann, A., Montoya, M., Murakami, S., Nawrath, S., Oka, A., Peltier, W. R., Robitaille, D.  
20 Y., Sokolev, A., Vettoretti, G., and Weber, S. L.: Investigating the causes of the response of the thermohaline circulation to past and future climate changes, *J. Climate*, 19, 1365–1387, 2006.
- Tarasov, L. and Peltier, R.: Greenland glacial history, borehole constraints, and Eemian extent, *J. Geophys. Res.*, 108, 2143, doi:10.1029/2001JB001731, 2003.
- 25 Thomas, A. L., Henderson, G. M., Deschamps, P., Yokoyama, Y., Mason, A. J., Bard, E., Hamelin, B., Durand, N., and Camoin, G.: Penultimate deglacial sea-level timing from uranium/thorium dating of Tahitian corals, *Science*, 324, 1186–1189, 2009.
- Venz, K. A., Hodell, D. A., Stanton, C., and Warnke, D. A.: A 1.0 Myr record of Glacial North  
30 Atlantic Intermediate Water variability from ODP site 982 in the northeast Atlantic, *Paleoceanography*, 14, 42–52, 1999.

[Title Page](#)[Abstract](#)[Introduction](#)[Conclusions](#)[References](#)[Tables](#)[Figures](#)[⏪](#)[⏩](#)[◀](#)[▶](#)[Back](#)[Close](#)[Full Screen / Esc](#)[Printer-friendly Version](#)[Interactive Discussion](#)

Wang, Y. J., Cheng, H., Edwards, R. L., An, Z. S., Wu, J. Y., Shen, C.-C., and Dorale, J. A.: A high-resolution absolute dated Late Pleistocene monsoon record from Hulu Cave, China, *Science*, 294, 2345–2348, 2001.

Williamson, M. S., Lenton, T. M., Shepherd, J. G., and Edwards, N. R.: An efficient terrestrial scheme (ENTS) for Earth system modelling, *Ecol. Model.*, 198, 362–374, 2006.

Wolff, E. W., Fischer, H., and Röthlisberger, R.: Glacial terminations as southern warmings without northern control, *Nat. Geosci.*, 2, 206–209, 2009.

CPD

5, 2555–2575, 2009

## Interhemispheric coupling and warm Antarctic interglacials

P. B. Holden et al.

Title Page

Abstract

Introduction

Conclusions

References

Tables

Figures

◀

▶

◀

▶

Back

Close

Full Screen / Esc

Printer-friendly Version

Interactive Discussion

## Interhemispheric coupling and warm Antarctic interglacials

P. B. Holden et al.

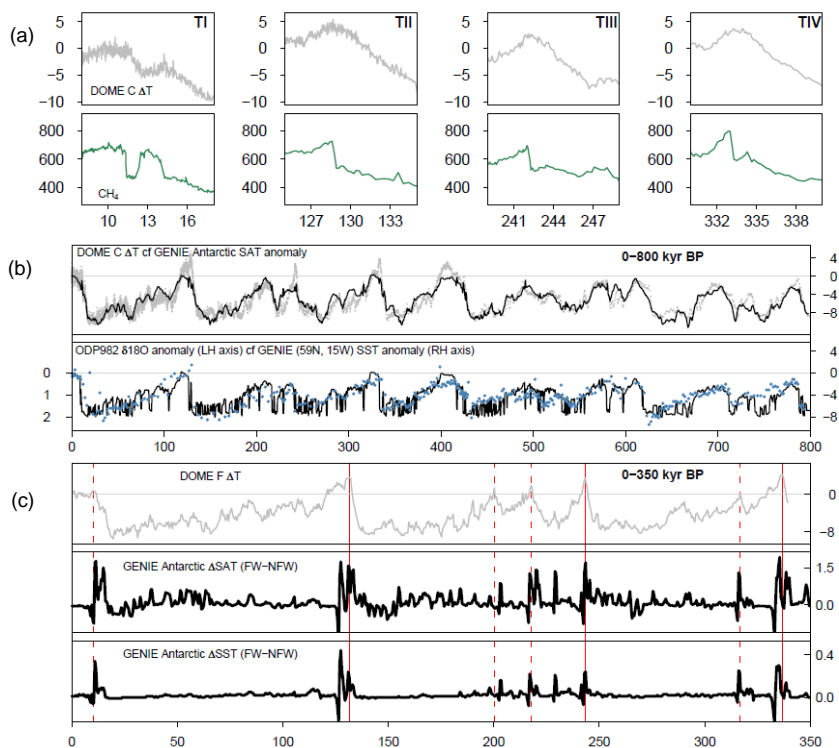


**Fig. 1.** (a) DOME C  $\delta D$ -inferred Antarctic temperature anomaly (Jouzel et al., 2007) (grey) and atmospheric CH<sub>4</sub> concentration (Louergue et al., 2008) (green) at the last four terminations. (b) 800 kyr records of DOME C Antarctic temperature anomaly (grey) and planktonic  $\delta^{18}\text{O}$  (blue) at ODP site 982 (57.3° N, 15.5° W) (Venz et al., 1999), compared respectively with the GENIE-1 (G<sub>FW</sub>) Antarctic SAT anomaly and the SST anomaly at the grid cell centred on 59° N, 15° W. (c) 350 kyr records of DOME F  $\delta D$ -inferred Antarctic temperature anomaly (Kawamura et al., 2007) (grey), GENIE-1 meltwater-induced (G<sub>FW</sub>–G<sub>NFW</sub>) Antarctic SAT and SST anomalies. Antarctic SAT is averaged over all Antarctica south of 71° S. Antarctic SST is averaged over all the Southern Ocean south of 62° S. Note: the simulation in (b) includes meltwater forcing, but the effects in Antarctica (up to ~1.5°C warming) are largely obscured by the larger changes across the terminations.

Title Page

Abstract

Introduction

Conclusions

References

Tables

Figures

◀

▶

◀

▶

Back

Close

Full Screen / Esc

Printer-friendly Version

Interactive Discussion

# Interhemispheric coupling and warm Antarctic interglacials

P. B. Holden et al.

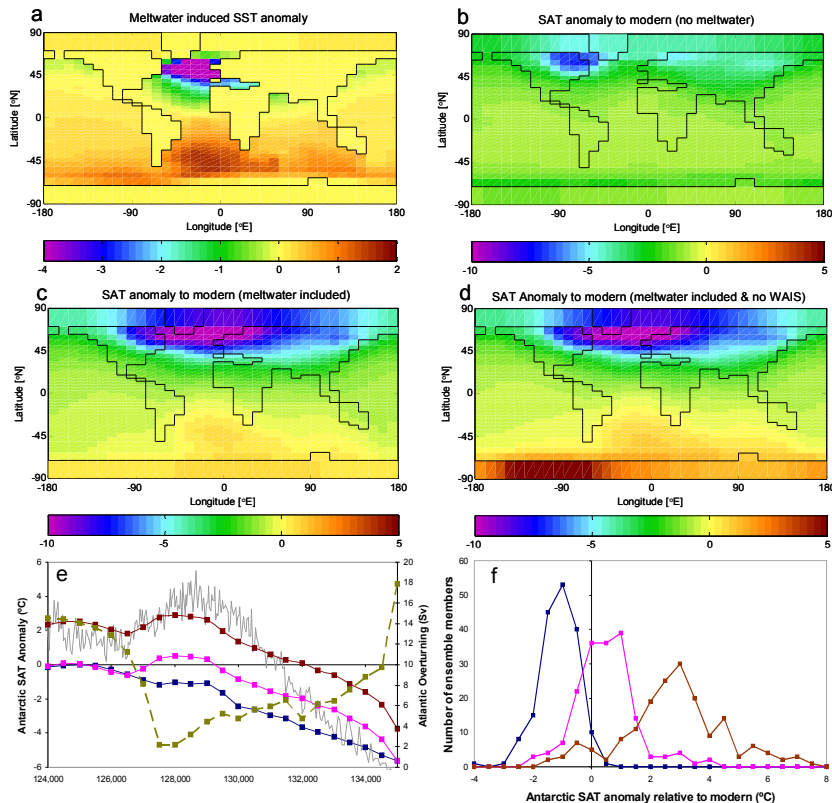


**Fig. 2.** GENIE-1 ensemble-averaged SST and SAT anomalies at 128 500 BP. Fields of (a) meltwater induced SST anomaly ( $E_{FW}-E_{NFW}$ ), and (b, c, d) SAT anomalies relative to an equilibrium pre-industrial ensemble  $E_M$  with (b) no meltwater flux ( $E_{NFW}-E_M$ ), (c) including Laurentide and Eurasian meltwater fluxes ( $E_{FW}-E_M$ ) and (d) including Laurentide and Eurasian meltwater fluxes and replacing West Antarctic Ice Sheet with land at sea-level ( $E_{WAIS}-E_M$ ). (e) Ensemble-averaged temporal behaviour of Antarctic SAT anomaly. The dashed green line is the ensemble-averaged ( $E_{FW}$ ) Atlantic overturning (maximum streamfunction at depths below 400 m). The grey line is the DOME C deuterium inferred anomaly (Jouzel et al., 2007). (f) Ensemble distributions of Antarctic SAT anomaly at 128 500 BP. Blue: no meltwater forcing ( $E_{NFW}-E_M$ ). Pink: meltwater forcing included ( $E_{FW}-E_M$ ). Brown: meltwater forcing included and WAIS removed to land at sea level ( $E_{WAIS}-E_M$ ).

Title Page

Abstract

Introduction

Conclusions

References

Tables

Figures

◀

▶

◀

▶

Back

Close

Full Screen / Esc

Printer-friendly Version

Interactive Discussion

## Interhemispheric coupling and warm Antarctic interglacials

P. B. Holden et al.

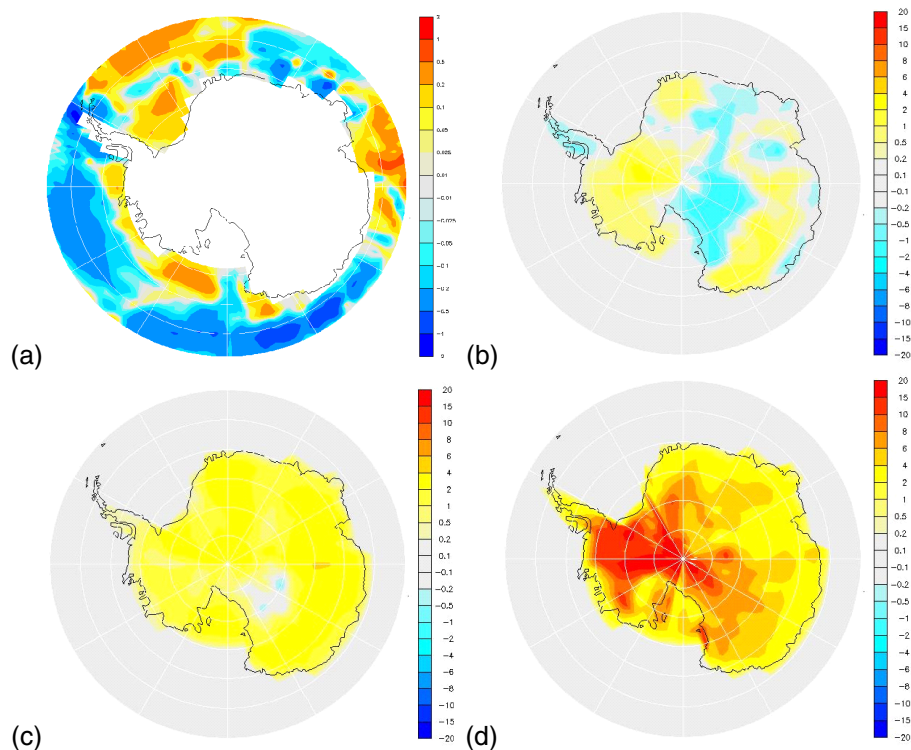


**Fig. 3.** HadCM3 SST and SAT anomalies at 130 000 BP. **(a)** Southern summer freshwater-induced SST anomaly due to 1 Sv North Atlantic hosing applied uniformly between 50–70° N ( $H_{FW} - H_{NFW}$ ). **(b, c, d)** Precipitation-weighted SAT anomalies relative to pre-industrial **(b)** with no hosing ( $H_{NFW} - H_M$ ), **(c)** including hosing ( $H_{FW} - H_M$ ), **(d)** including hosing and with WAIS removed to land at 200 m ( $H_{WAIS} - H_M$ ).

Title Page

Abstract

Introduction

Conclusions

References

Tables

Figures

⏪

⏩

◀

▶

Back

Close

Full Screen / Esc

Printer-friendly Version

Interactive Discussion